16th World Conference on Earthquake Engineering, 16WCEE 2017
Santiago Chile, January 9th to 13th 2017
Paper N° 3611 (Abstract ID)
Registration Code: S- J1463141579

NEW EMULATION-BASED APPROACH FOR PROBABILISTIC SEISMIC DEMAND

S. Minas[(1)], R.E. Chandler[(2)] and T. Rossetto[(3)]

[(1)] EngD student, University College of London, s.minas@ucl.ac.uk
[(2)] Professor, University College of London, r.chandler@ucl.ac.uk
[(3)] Professor, University College of London, t.rossetto@ucl.ac.uk

Abstract

An advanced statistical emulation-based approach to compute the probabilistic seismic demand is introduced here. The emulation approach, which is a version of kriging, uses a mean function as a first approximation of the mean conditional distribution of Engineering Demand Parameter given Intensity Measure (EDP|IM) and then models the approximation errors as a Gaussian Process (GP). The main advantage of the kriging emulator is its flexibility, as it does not impose a fixed mathematical form on the EDP|IM relationship as in other approaches (i.e. standard cloud method). In this study, a case-study building representing the Special-Code vulnerability class, is analyzed at a high level of fidelity, namely nonlinear dynamic analysis. For the evaluation of the emulator, two different scenarios are considered, each corresponding to a different "assumed reality" represented by an artificially generated IM:EDP relationship derived from the sample of real analysis data. These "assumed realities" are used as a reference point to assess the performance of the emulation-based approach, and to compare against the outcomes of the standard cloud analysis. A number of input configurations are tested, utilizing two sampling processes (i.e. random and stratified sampling) and varying the number of training inputs. The outcomes of the current work show that the proposed statistical emulation-based approach, when calibrated with high fidelity analysis data and combined with the advanced IM I_{Np}, outperforms the standard cloud method in terms of coverage probability and average length, while insignificant differences are obtained in the mean squared error estimations (MSE). The improved performance of emulator over the cloud method is maintained in both "assumed realities" tested showing the capability of the former approach to better estimate the EDP|IM relationship for the cases that does necessarily follow a favorable pattern (e.g. power-law).

Keywords: probabilistic seismic demand; statistical emulation; kriging;

1. Introduction

Fragility functions constitute an essential component of the Performance-based earthquake engineering (PBEE) framework [1]. In the current state-of-the-art, there are three main methods for deriving fragility functions: empirical, analytical and based on experts' judgement [2]. The former approach is considered to be the most credible one, while the latter is only used when none of the other two approaches can be implemented [3]. However, empirical approaches have several limitations, including the difficulty in properly characterizing the levels of seismic intensity and a non-subjective damage state allocation; but more importantly, the lack of sufficient seismic damage data in most areas of the world.

Analytical methods are becoming increasingly popular as they offer the user the flexibility to choose from analysis methodologies, various structural parameters, characteristics of input ground motions etc. Several approaches exist for the analytical fragility assessment of various building classes. The present study aims to advance methods and tools for analytical fragility analysis of mid-rise RC buildings. This is achieved by investigating alternative statistical approaches for fitting the conditional distribution of Engineering Demand Parameter given Intensity Measure (EDP|IM) to be used for the derivation of fragility curves. In particular, emulation surrogate models are adopted to provide estimates, and the associated variances, for the conditional distribution of EDP|IM relationship that would be obtained if it was possible to run the analysis models at all

possible combinations of their inputs, i.e. any possible ground motion input. The emulation approach, which is a version of kriging, uses a mean function as a first approximation of the mean conditional distribution and then models the approximation errors as a Gaussian Process (GP). The main advantage is the flexibility associated with this approach, as it does not impose a fixed mathematical form on the EDP|IM relationship as in the standard cloud method (discussed below).

A new statistical emulation approach which provides estimates and variances, for the conditional distribution of EDP|IM relationship is introduced here, as a part of a wider analytical fragility assessment framework. The capabilities of this new approach are investigated when trying to predict two artificially generated 'true' functions and tested against the outcomes of the standard cloud analysis.

2. Cloud analysis

One of the most commonly used methods for characterizing the relationship between EDP and IM is the cloud method [4–6]. Within this method, a structure is subjected to a series of ground motion (GM) time-histories associated with respective IM values in order to estimate the associated seismic response. Nonlinear dynamic analysis (e.g. nonlinear time-history analysis - NLTHA), is usually used to estimate the response of the building, expressed in terms of EDP, when subjected to the aforementioned GMs. The resultant peak values of EDP for given IM levels when recorded form a scatter of points, the so-called "cloud". A statistical regression model is used to fit the cloud of data points which is represented by a simple power-law model. According to this model, the EDP is considered to vary roughly as a power-law of the form aIM^b such that, after taking logarithms, the relationship can be expressed as in equation (1):

$$\ln(EDP) = \ln(a) + b\ln(IM) + e \tag{1}$$

where EDP is the conditional median of the demand given the IM, a, b are the parameters of the regression, and e is a zero mean random variable representing the variability of $\ln(EDP)$ given the IM. However, some situations exhibit substantial heteroskedasticity (i.e. non-constant variance), which needs to be modelled explicitly within the fragility analysis framework [7]; for example by performing linear regressions locally in a region of IM values of interest. The use of logarithmic transformation indicates that the EDPs are assumed to be lognormally distributed conditional upon the values of the IMs; this is a common assumption that has been confirmed as reasonable in many past studies [8,9].

Apart from the advantages of simplicity and rapidity over alternative demand fragility assessment methods, discussed in following sections, cloud analysis has several restrictions. Firstly, the assumption that the relation of IM and EDP is represented appropriately by a linear model in the log space. This assumption may be valid for a short range of IM and EDP combinations but not for the entire cloud response space. Secondly, the dispersion of the probability distribution of EDP given IM is constant, while several studies have shown that the dispersion of EDP might increase for increasing IM values [10]. Lastly, the accuracy of the cloud method is highly dependent on the selection of earthquake records used as an input [11].

3. Statistical emulation

Complex mathematical models exist in all scientific and engineering areas aiming to capture the real-world processes and simulate sufficiently the real-systems. These mathematical models are usually translated into computer codes and may require significant computational resources. The mathematical functions and the related computer codes may be referred to as simulators [12]. A simulator, as a function $f(.)$, takes deterministic vectors of inputs $\mathbf{x}$ and generates unique outputs, $\mathbf{y} = f(\mathbf{x})$ for each given input. However, the results are subject to uncertainties – for example, due to uncertainties in the inputs and in the simulator construction itself [13]. To assess the effect of these uncertainties, one option is to use uncertainty and sensitivity analysis methods requiring many simulator runs, as discussed at [14]. However, this is impractical for complex simulators that are computationally demanding to run [12]. To overcome this, an approximation $\hat{f}(\mathbf{x})$ of the simulator $f(\mathbf{x})$,

known as a statistical emulator, may be introduced to act as a surrogate. If $\hat{f}(\mathbf{x})$ is a good proxy of the simulator, it can be used to carry out uncertainty and sensitivity analysis but with significantly less effort.

An emulator is a simple statistical representation of the simulator and is used for the rapid estimation of the simulation outputs. The emulator provides an approximation, $\hat{f}(\mathbf{x})$ say, to the true simulator output $f(\mathbf{x})$; and also provides a standard deviation to quantify the associated approximation error. A small number of data points, obtained by running the simulator at carefully chosen configurations of the inputs, is required to train the emulator. The emulator developed for the present study is a Gaussian process (GP) model. GP models are described in the next subsection; and contrasted with the standard approach of cloud analysis in Section 2.

In the standard GP approach to the modelling of simulator outputs, the output function $f(\mathbf{x})$ is regarded as a realized value of a random process such that the outputs at distinct values of **x** jointly follow a normal (or Gaussian) distribution. In most applications, $f(\mathbf{x})$ is a 'smooth' function in the sense that a small variation in the input **x** will result in a small perturbation in the output $f(\mathbf{x})$. Smoothness of a Gaussian process is ensured by specifying an appropriate structure for the covariance between process values at distinct values of **x**. For example, the use of a Gaussian covariance model (not to be confused with the "Gaussian" in the GP, which relates to the distribution, rather than the covariance structure), results in smooth realizations that are infinitely differentiable.

In the context of analytical fragility estimation, the input **x** represents a ground motion sequence and the output $f(\mathbf{x})$ represents the simulated EDP for that sequence. However, fragility estimates are rarely presented as functions of an entire ground motion sequence: rather, they are presented as a function of an intensity measure $t = t(\mathbf{x})$, say, that is used as a proxy for the complete sequence. In practice, the relationship between any such scalar proxy measure and the EDP is imperfect so that the simulator outputs, regarded as a function of *t* rather than **x**, are no longer smooth. As an example of this, two different ground motion records characterized by the same value of *t* (i.e. having the same IM) will not in general generate identical outputs. As a result, the standard emulation approach must be modified slightly to apply it in the context of fragility estimation.

The required modification is still to regard $f(\mathbf{x})$ as the realized value of a random process, but now such that the conditional distributions of $f(\mathbf{x})$ given $t(\mathbf{x})$ themselves form a Gaussian process. Specifically, write $f(\mathbf{x})$ as:

$$f(\mathbf{x}) = \mu(t) + \varepsilon(\mathbf{x}) \tag{2}$$

where $\mu(t)$ represents the systematic variation of the output with the IM and $\varepsilon(\mathbf{x})$ is a discrepancy term with $E[\varepsilon(\mathbf{x})] = 0$, representing uncertainty due to the fact that t does not fully capture the relevant information in $\mathbf{x}$. In the first instance it will be convenient to assume that $\varepsilon(\mathbf{x})$ is normally distributed with a constant variance, τ^2 (this assumption can be checked when applying the methodology); also that $\varepsilon(\mathbf{x})$ is independent of $\mu(t)$, and that $\varepsilon(\mathbf{x}_1)$ is independent of $\varepsilon(\mathbf{x}_2)$ when $\mathbf{x}_1 \neq \mathbf{x}_2$. Note that in equation (2), the term $\varepsilon(\mathbf{x})$ is deliberately used instead of $\varepsilon(t)$. The reason for doing this is to allow two simulator outputs with different $\mathbf{x}$ but same value of t, to be considered as separate, allowing for scatter about the overall mean curve in a plot of $f(\mathbf{x})$ against $t(\mathbf{x})$. Equation (2) then immediately yields the conditional distribution of EDP given IM as normal, with expected value $\mu(IM)$ and variance τ^2.

To exploit GP emulation methodology now, a final additional assumption is that $\mu(t)$ varies smoothly with *t* and hence can itself be considered as a realization of a GP. Specifically, denote the expected value of $\mu(t)$ by $m(t)$, denote its variance by σ^2 and specify a correlation function (such as the Gaussian) that ensures smooth variation with *t*. Under the Gaussian correlation function, the covariance between $\mu(t_1)$ and $\mu(t_2)$ is:

$$\sigma^2 \exp\left[-\frac{(t_1-t_2)^2}{2\delta^2}\right] \tag{3}$$

where δ is a parameter controlling the rate of decay of the correlation between function values at increasingly separated values of t. As an illustrative example, the mean function $m(t)$ could be specified as linear, i.e. $m(t)=\beta_0+\beta_1 t$: this represents a first approximation to the function $\mu(t)$ in Eq.(2), with the correlation structure allowing for smooth variation in the "approximation error" $\mu(t)-m(t)=z(t)$, say.

Combining all of the above, in the case where the mean function $m(t)$ is linear we find that values of $f(\mathbf{x})$ at distinct values of $\mathbf{x}$ are jointly normally distributed such that:

- The expected value of $f(\mathbf{x})$ is: $\beta_0+\beta_1 t$
- The variance of $f(\mathbf{x})$ is equal to: $\mathrm{Var}[\mu(t)]+\mathrm{Var}[\varepsilon(\mathbf{x})]=\sigma^2+\tau^2$
- For $\mathbf{x}_1 \neq \mathbf{x}_2$, the covariance between $f(\mathbf{x}_1)$ and $f(\mathbf{x}_2)$ is:

$$\begin{aligned}\mathrm{Cov}[f(\mathbf{x}_1), f(\mathbf{x}_2)] &= \mathrm{Cov}[\mu(t_1)+\varepsilon(\mathbf{x}_1), \mu(t_2)+\varepsilon(\mathbf{x}_2)] \\ &= \mathrm{Cov}[\mu(t_1), \mu(t_2)] = \sigma^2 \exp\left[-\frac{(t_1-t_2)^2}{2\delta^2}\right]\end{aligned} \tag{4}$$

where $t_1=t(\mathbf{x}_1)$ and $t_2=t(\mathbf{x}_2)$.

Notice that these expressions depend on the full input vector $\mathbf{x}$ only through the IM $t(\mathbf{x})$. As a result, the simulator outputs can be analyzed as though they are functions of t alone and, specifically, subjected to a standard GP analysis to estimate the systematic variation $\mu(t)$. The only difference between this formulation and a standard GP emulation problem is that when $t_1=t_2$, the covariance between the simulator outputs is $\sigma^2+\tau^2$ rather than just σ^2. The additional τ^2 term allows for additional variance associated with the discrepancy term $\varepsilon(\mathbf{x})$ in equation (2).

Having formulated the problem in terms of Gaussian processes, the simulator can be run a few times at different values of $\mathbf{x}$, and the resulting outputs can be used to estimate the parameters in the GP model which, as set out above, are the regression coefficients β_0 and β_1, the variances σ^2 and τ^2, and the correlation decay parameter δ. Having estimated the parameters, the results can be used to interpolate optimally between the existing simulator runs so as to construct an estimate of the demand curve $\mu(t)$ and associated standard deviation. The optimal interpolation relies on standard results for calculating conditional distributions in a Gaussian framework. The approach is used extensively in geostatistics to interpolate between observations made at different spatial locations, where it is often referred to as "kriging" [15]. In geostatistics, the term τ^2 is referred to as a 'nugget' and accounts for local-scale variation or measurement error. Nonetheless, in the present context the above argument shows that it can be derived purely by considering the structure of the probabilistic seismic demand problem.

It is noteworthy to mention that similarly to the cloud method, the emulator analysis is also carried in terms of $\ln(EDP)$, due to the normality and heteroscedasticity assumptions, which are better justified on the log scale.

4. Methodology

4.1 Defining 'true' functions

In this study two different scenarios are considered, each corresponding to a different "reality" represented by an artificially generated IM:EDP relationship derived from a sample of real analysis data, as described in Section 4.3. In each relationship, the expected value of some function of the EDP is given by a mean function $\mu(t)$ as in equation (2); and $\mu(t)$ is represented as a sum of a deterministic mean function $m(t)$ and an approximation error $z(t)$:

$$\mu(t) = m(t) + z(t) \tag{5}$$

The deterministic mean function $m(t)$ is represented by a simple regression model. Traditional cloud analysis corresponds to a situation in which $\mu(t)$ is the expected value of $\ln(EDP)$, the mean function $m(t)$ is a linear function of $\ln(t)$ and the approximation error $z(t)$ is zero. However, the framework considered here allows an exploration of a wider range of situations.

Our two chosen "assumed realities" are as follows:

1. Reality 1: the expected value of $\ln(EDP)$ is an exact linear function of $\ln(IM)$ with no approximation error (i.e. with $z(t) = 0$ in equation (5)). This "assumed reality" is the situation for which the standard cloud method is designed.
2. Reality 2: the function $\mu(t)$ represents the expected value of EDP rather than $\ln(EDP)$, and a non-zero approximation error $z(t)$ is included in equation (5) so that $\mu(t)$ is no longer an exact linear function of $\ln(t)$. The approximation error is generated as a Gaussian random field (making sure that the resultant "true" function is monotonically increasing). This case can be used as an example where both models (standard and emulator) are wrong, and will shed light to the capability of these two models to estimate the EDP|IM relationship.

The two generated true functions are illustrated in Figure 1. As it becomes evident from the description of each "assumed reality", the objective is to explore the capability of the methods to predict EDP|IM relationship under favorable or less favorable situations. This is done by using a subset of the generated EDMs to calibrate both the traditional and emulator methods, and then using the results to predict the remainder of the generated EDMs. As well as predicting the values themselves, 95% prediction intervals are computed as a way of quantifying the uncertainty in the predictions.

To this aim, the coverage probability of the 95% prediction intervals (hereafter called coverage), the average length of these intervals and the mean squared error (MSE) are the metrics used to assess the performance of the emulation and standard approach. Coverage shows how accurate the uncertainty assessment is, by calculating the proportion of intervals containing the actual EDP. If the uncertainty assessment is accurate, the coverages from a method should be equal to their nominal value of 0.95.

The average interval length assesses the amount of uncertainty in the predictions intervals and is computed as:

$$\text{Average Length} = \sum_{i=1}^{n}\left(\frac{UL95_i - LL95_i}{n}\right) \tag{6}$$

where $UL95_i$ and $LL95_i$ are respectively the upper and lower ends of the ith prediction interval. Ideally, prediction intervals should be as short as possible subject to the correct coverage.

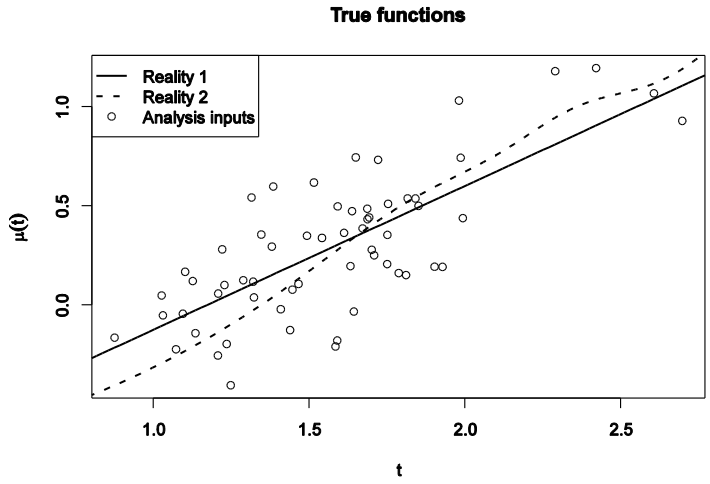

Figure 1 - Two artificially generated "true" functions for the high-fidelity analysis of the Special-Code case study.

The MSE assesses empirically the quality of the vector of n predictions, $\hat{Y}$, with respect to an simulated EDP, Y, and is defined as:

$$MSE = \frac{1}{n}\sum_{i=1}^{n}\left(\hat{Y}_i - Y_i\right)^2 \tag{7}$$

4.2 Tailoring emulator – Preparation and training

A case study building design is analyzed at a high level of fidelity, as discussed in detail in Section 4.3. The resultant dataset, expressed in terms of IM and EDP is used as the input to train the emulator in order to provide estimates and variances, for the conditional distribution of EDP|IM relationship. To this aim, a computer code implementing the proposed framework is scripted in R [16].

The full sample is split to a training set and a test set. Four different cases are investigated, three utilizing training samples of 10, 25, 50 training inputs, representing a small, medium and large sample, and one using the full training input sample consisting of number of points associated with the ground motions that push the structures to nonlinear range [17]. Regarding the reduced samples, two sampling strategies are considered, including a random sampling, and a stratified sampling approach. For the stratified sampling, the full input sample is divided into 5 strata (bins) of equal intensity measure width, and then random sampling is applied to select the user-specified number of inputs (e.g. 2, 5, 10 inputs from each bin).

Following the sampling procedure, the selected inputs are then used to train the emulator. As stated in previous sections, the setup of the emulation model allows one to implement a regression model to describe the mean function $\mu(t)$ and is suitable for the nature of the problem of interest. In this study, the authors decided to maintain a power-law regression model, as in the standard cloud method; however, alternative models, such as linear or higher order polynomials may also be used.

The covariance parameters, as well as the nugget are estimated by using the variofit() function, which is included in the geoR package [18]. Ordinary least squares is used to fit the covariance model to an empirical variogram: the Gaussian model is used in the present work. The resultant covariance parameters are then used to predict the remaining EDPs and to calculate the 95% prediction intervals.

4.3 Case study structure and ground motion selection

A regular reinforced concrete (RC) moment resisting frame (MRF) is modelled and implemented as a case study for the current research work. This structure is designed according to the latest Italian seismic code (or NIBC08; [19]), fully consistent with Eurocode 8 (EC8; [20]), following the High Ductility Class (DCH) rules, and

represents the Special-Code vulnerability class, hereafter called the Special-Code building. Interstorey heights, span of each bay and cross-sections dimensions for the case-study building are reported in Figure 2. The considered frame is regular (in plan and elevation). Details regarding the design and the modelling of the building are available in [21] and [17].

Static pushover (PO) analysis is carried out by applying increments of lateral loads to the side nodes of the structure. These lateral loads are proportionally distributed with respect to the interstorey heights (triangular distribution). The PO analysis is carried out until a predefined target displacement is reached, corresponding to the expected collapse state.

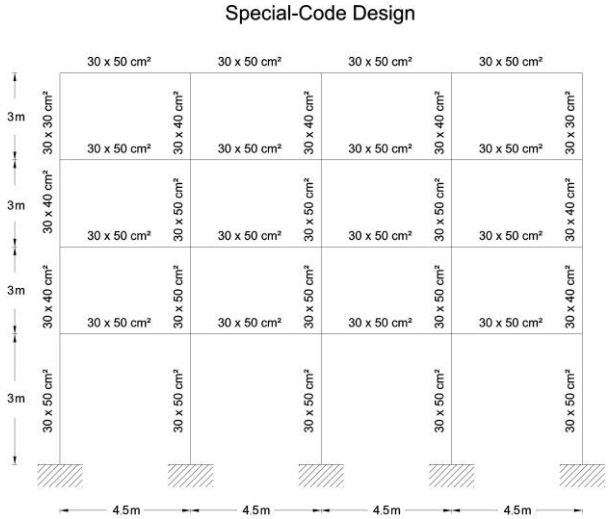

Figure 2 - Elevation dimensions and member cross-sections of the Special-Code RC frame.

Table 1 summarizes the structural and dynamic properties associated with the case-study building model, namely mass of the system *m*, fundamental period T_1 as well as the modal mass participation at the first mode of vibration.

Table 1 - Structural and dynamic properties of the case-study building.

Building Type	Total mass, m (tn)	T_1 (s)	Modal Mass Participation (1st Mode)
Special-Code	172.9	0.506	92.8 %

Figure 3 shows the static PO curve associated with the studied building, and is reported in terms of top center-of-mass displacement divided by the total height of the structure (i.e., the roof drift ratio, RDR) along the horizontal axis of the diagram, and base shear divided by the building's seismic weight along the vertical axis (i.e., base shear coefficient).

A set of 150 unscaled ground motion records from the SIMBAD database (Selected Input Motions for displacement-Based Assessment and Design; [22]), is used here. SIMBAD includes a total of 467 tri-axial accelerograms, consisting of two horizontal (X-Y) and one vertical (Z) components, generated by 130 worldwide seismic events (including main shocks and aftershocks). In particular, the database includes shallow crustal earthquakes with moment magnitudes (M_w) ranging from 5 to 7.3 and epicentral distances $R \leq 35$ km. A subset of 150 records is considered here to provide a significant number of strong-motion records of engineering relevance for the applications presented in this paper. These records are selected by first ranking the 467 records in terms of their PGA values (by using the geometric mean of the two horizontal components) and then keeping the component with the largest PGA value (for the 150 stations with highest mean PGA).

Nonlinear Dynamic Procedures (NDP), and particularly NLTHA is utilized to estimate the seismic response of the studied frame, representing a high level of fidelity analysis, namely high fidelity.

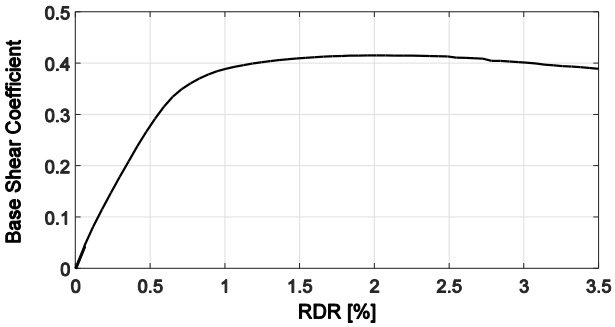

Figure 3 - Static PO curve for the Special-Code RC frame building.

In the current study, the focus is laid on the deformation-based EDP, defined as maximum (over all stories) peak interstorey drift ratio (denoted as MIDR).
With regard to the IM input, previous studies agree that most informative IMs (i.e. vector-valued and advanced IMs respectively) are more suitable for predicting the seismic response of structure, and eventually the seismic fragility [17,23], as they also perform well under most IM selection criteria. Therefore the advanced scalar IM I_{Np} [24] is used herein. I_{Np}, which is based on the spectral ordinate $Sa(T_1)$ and the parameter N_p, is defined as:

$$I_{N_p} = S_a(T_1) N_p^{\alpha} \tag{8}$$

where α parameter is assumed to be α = 0.4 based on the tests conducted by the authors and N_p is defined as:

$$N_p = \frac{S_{a,avg}(T_1,...,T_N)}{S_a(T_1)} = \frac{\left[\prod_i^N S_a(T_i)\right]^{1/N}}{S_a(T_1)} \tag{9}$$

T_N corresponds to the maximum period of interest and lays within a range of 2 and 2.5T_1, as suggested by the authors.

5. Evaluation of emulation for probabilistic seismic demand against cloud analysis

All the steps discussed in the Methodology section are applied here in order to build the emulator, which provides estimates, and the associated variances, for the conditional distribution of EDP|IM relationship. The outcomes of the emulation approach are then compared to standard method outcomes, namely the cloud method. The results of the NDA analysis of the Special-Code building, expressed in terms of MIDR and the advanced IM, I_{Np} are presented here. The reason for selecting this EDP:IM combination is based on previous studies carried by the authors regarding the selection of optimal IMs for the fragility analysis of mid-rise RC buildings [17].

Figure 4 illustrates the mean estimations and the associated 95% confidence intervals of the emulation and cloud approach, utilizing the full sample for the two "assumed realities" defined in Section 4.1. Table 2 shows the training inputs of the emulator, namely the sample size (stratified sampling used here) and the covariance model, in conjunction with the metrics used to assess the performance of the emulation and the cloud approach, for the two "assumed realities" investigated. A close examination of the results presented in Table 2 shows that the coverage probability for the case of the emulator is always closely matching the nominal coverage probability, with ±0.5% difference for both generated true functions, while the associated difference for the cloud case is reaching up to +3.3%. This means that the cloud approach is producing conservative confidence intervals, i.e. wider confidence intervals. As a result, the estimated average length of the emulation approach is always less

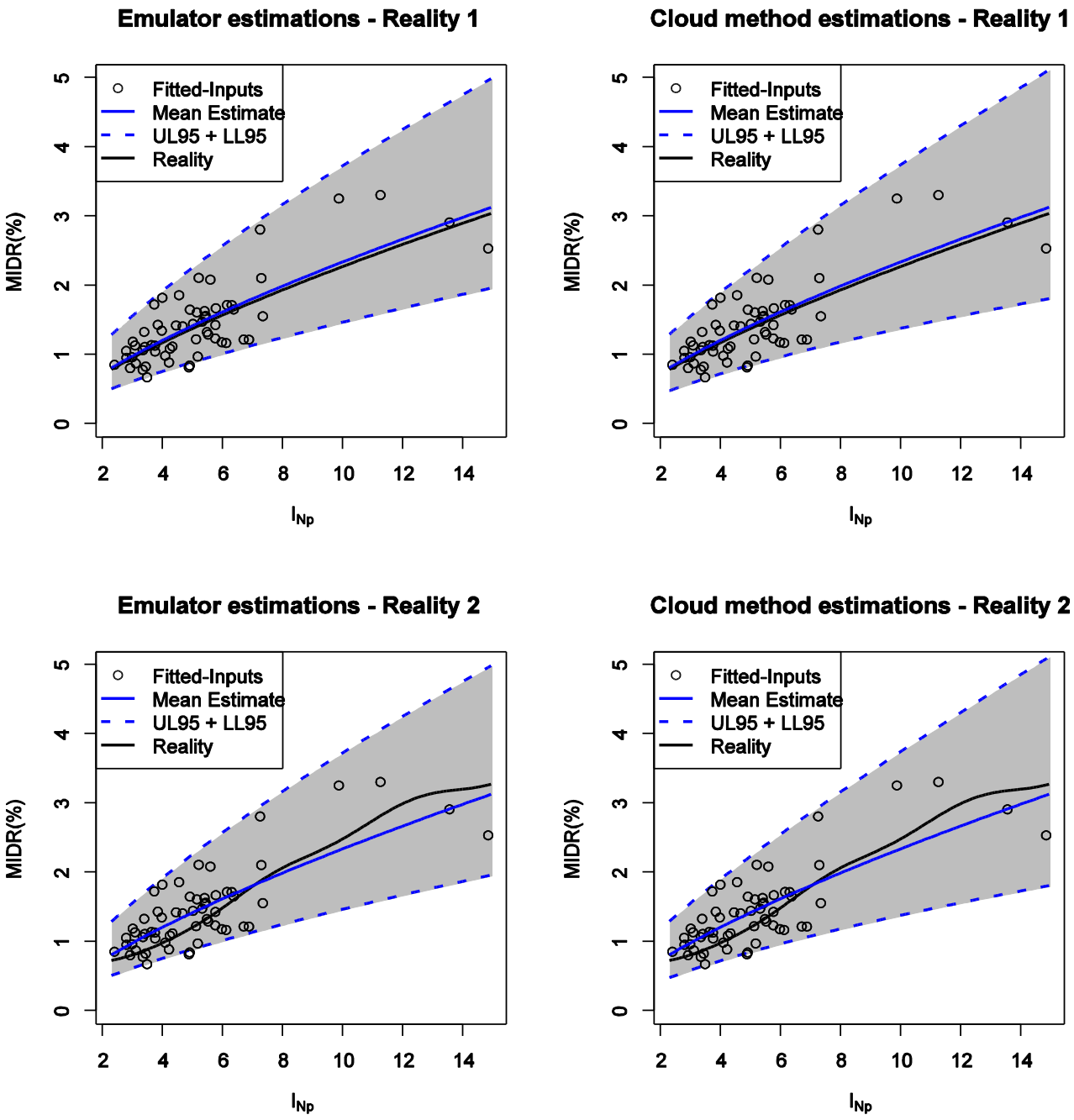

Figure 4 - Mean estimations and associated 95% confidence intervals of emulation (left panels) and the cloud approach (right panels) for Reality 1 (top row) and Reality 2 (bottom row).

than the respective average length of the cloud, indicating that the predictions of the emulator are less uncertain. The reduction of the average length recorded in the case of emulator (comparing to cloud) is between 4.0-6.7% for larger sample sizes (i.e. full and 50-points sample), and 10.5-13.6% smaller sample sizes (25- and 10-points sample). Note that the biggest differences in average length are observed for the Reality 2, showing the capability of the emulator to better estimate the EDP|IM relationship for the cases that does necessarily follow a favorable pattern (e.g. power-law). Last, insignificant differences are obtained in terms of the MSE computed for both for models, with the difference never exceeding ±1.7% for Realities 2, and ±3.3% for Reality 1.

Table 2 - Emulator's inputs and metrics to assess the performance of the emulation and the cloud approach.

Sample size	Covariance Model	Reality	MSE Emulator	MSE Cloud	Average Length Emulator	Average Length Cloud	Coverage (%) Emulator	Coverage (%) Cloud
Full	Gaussian	1	0.397	0.410	1.657	1.722	95.00	98.33
50	Gaussian	1	1.004	1.019	1.653	1.743	95.18	97.44
25	Gaussian	1	4.245	4.159	1.689	1.866	94.60	96.72
10	Gaussian	1	4.352	4.238	1.696	1.886	94.89	97.08
Full	Gaussian	2	4.717	4.692	1.989	2.087	95.00	98.33
50	Gaussian	2	5.050	5.035	1.982	2.114	95.14	97.44
25	Gaussian	2	8.931	9.086	1.996	2.268	94.54	97.01
10	Gaussian	2	8.555	8.513	2.026	2.284	94.45	96.65

6. Conclusions and future work

In this study, a new statistical emulation approach is introduced for estimating the mean and the associated variance of the conditional distribution of EDP|IM relationship, overcoming some limitations of the standard cloud method. The capabilities of this new approach are investigated when trying to predict different "assumed realities" and the results are compared against the standard cloud analysis results.

To this aim, a RC mid-rise building representing the Special-Code vulnerability class of the Italian building stock is used as a case-study structure. An artificially generated IM:EDP relationships derived from a sample of real analysis data, obtained from the aforementioned case-study building, is considered. In addition, various sampling strategies and covariance structures are also explored in order to shed light to the capabilities of the emulator under different conditions. Random sampling strategy showed significant sensitivity to the selection of training inputs, especially for the cases of smaller sample sizes; as a result, stratified sampling is used here.

In the presented case study, the coverage probability for the proposed emulation model is always closely matching the nominal coverage probability and also resulting a significant reduction of the average length, comparing to the respective average length of the cloud method. Particularly for the Reality 2 case, the average length reduction reaches 13.6%, highlighting the flexibility of the emulator over the standard approach.

As a part of an ongoing research work, the proposed methodology has been also applied to case-studies associated with numerous input variations. These variations include the employment of buildings of different vulnerability class (i.e. Pre-Code buildings), the choice of additional scalar IMs (i.e. peak ground acceleration (*PGA*), spectral acceleration $Sa(T_1)$ amongst others), and the implementation of different levels of analysis fidelity (i.e. low-fidelity analysis, based on simplified analysis methods, such as the variant of capacity spectrum method, FRACAS[25]). The kriging exploits the relationship of neighboring points of the data sample, explaining why this approach is better suited with advanced IMs, as the scatter relation is reduced. However, applying the emulator to a wider scatter (e.g. low-fidelity results expressed in terms of peak ground parameters), may not always provide improvements that justify the additional work required. As a result, the future steps of this work will explore the full potential of this approach by employing a Bayesian framework to account for the uncertainty related to the emulator's covariance parameters. Furthermore, further validation will be carried out, investigating more rigorous ground motion selection procedures, and additional building case studies (i.e. RC buildings with infills).

Acknowledgements

Funding for this research work has been provided by the Engineering and Physical Sciences Research Council (EPSRC) in the UK and the AIR Worldwide Ltd through the Urban Sustainability and Resilience program at University College London.

7. References

[1] Deierlein GG, Krawinkler H, Cornell CA. A framework for performance-based earthquake engineering. Pacific Conf Earthq Eng 2003;273:1–8. doi:10.1061/9780784412121.173.

[2] Porter K a, Farokhnia K, Cho IH, Grant D, Jaiswal K, Wald D. Global Vulnerability Estimation Methods for the Global Earthquake Model. 15th World Conf. Earthq. Eng., Lisbon, Portugal: 2012, p. 24–8.

[3] D'Ayala D, Meslem A, Vamvatsikos D, Porter K, Rossetto T, Crowley H, et al. Guidelines for Analytical Vulnerability Assessment of low-mid-rise Buildings – Methodology. Pavia, Italy: GEM Foundation; 2013.

[4] Bazzurro P, Cornell CA, Shome N, Carballo JE. Three proposals for characterizing MDOF nonlinear seismic response. J Struct Eng 1998;124:1281–9. doi:Doi 10.1061/(Asce)0733-9445(1998)124:11(1281).

[5] Luco C, Cornell CA. Seismic drift demands for two SMRF structures with brittle connections. Structural Engineering World Wide. Struct Eng World Wide; Elsevier Sci Ltd, Oxford, Engl 1998:paper T158-3.

[6] Jalayer F. Direct probabilistic seismic analysis: implementing non-linear dynamic assessments. Stanford University, 2003.

[7] Modica A, Stafford PJ. Vector fragility surfaces for reinforced concrete frames in Europe. Bull Earthq Eng 2014;12:1725–53. doi:10.1007/s10518-013-9571-z.

[8] Ibarra LF, Krawinkler H. Global Collapse of Frame Structures under Seismic Excitations Global Collapse of Frame Structures under Seismic Excitations. Berkeley, California: 2005.

[9] Cornell CA, Jalayer F, Hamburger RO, Foutch DA. Probabilistic Basis for 2000 SAC Federal Emergency Management Agency Steel Moment Frame Guidelines. J Struct Eng 2002;128:526–33. doi:10.1061/(ASCE)0733-9445(2002)128:4(526).

[10] Vamvatsikos D, Cornell CA. Incremental dynamic analysis. Earthq Eng Struct Dyn 2002;31:491–514. doi:10.1002/eqe.141.

[11] Jalayer F, De Risi R, Manfredi G. Bayesian Cloud Analysis: efficient structural fragility assessment using linear regression. Bull Earthq Eng 2014;13:1183–203. doi:10.1007/s10518-014-9692-z.

[12] O'Hagan A. Bayesian analysis of computer code outputs: A tutorial. Reliab Eng Syst Saf 2006;91:1290–300. doi:10.1016/j.ress.2005.11.025.

[13] Kennedy MC, O'Hagan A. Bayesian Calibration of Computer Models. J R Stat Soc Ser B (Statistical Methodol 2001;63:425–64. doi:10.1111/1467-9868.00294.

[14] Saltelli A, Chan K, Scott E. Sensitivity analysis. Wiley series in probability and statistics. Chichester: Wiley; 2000.

[15] Sacks J, Welch WJ, Mitchell JSB, Henry PW. Design and Experiments of Computer Experiments. Stat Sci 1989;4:409–23.

[16] R Core Team. R: A language and environment for statistical computing. 2014.

[17] Minas S, Galasso C, Rossetto T. Spectral Shape Proxies and Simplified Fragility Analysis of Mid- Rise Reinforced Concrete Buildings. 12th Int. Conf. Appl. Stat. Probab. Civ. Eng. ICASP12, Vancouver, Canada: 2015, p. 1–8.

[18] Ribeiro Jr P, Diggle P. geoR: A package for geostatistical analysis. R-NEWS 2001;1:15–8.

[19] Decreto Ministeriale del 14/01/2008. Norme Tecniche per le Costruzioni. Rome: Gazzetta Ufficiale della Repubblica Italiana, 29.; 2008.

[20] EN 1998-1. Eurocode 8: Design of structures for earthquake resistance – Part 1: General rules, seismic actions and rules for buildings. The European Union Per Regulation 305/2011, Directive 98/34/EC, Directive2004/18/EC; 2004.

[21] De Luca F, Elefante L, Iervolino I, Verderame GM. Strutture esistenti e di nuova progettazione : comportamento sismico a confronto. Anidis 2009 XIII Convegno - L' Ing. Sismica Ital., Bologna: 2009.

[22] Smerzini C, Galasso C, Iervolino I, Paolucci R. Ground motion record selection based on broadband spectral compatibility. Earthq Spectra 2013;30:1427–48. doi:10.1193/052312EQS197M.

[23] Ebrahimian H, Jalayer F, Lucchini A, Mollaioli F, Manfredi G. Preliminary ranking of alternative scalar and vector intensity measures of ground shaking. Bull Earthq Eng 2015;13:2805–40. doi:10.1007/s10518-015-9755-9.

[24] Bojórquez E, Iervolino I. Spectral shape proxies and nonlinear structural response. Soil Dyn Earthq Eng 2011;31:996–1008. doi:10.1016/j.soildyn.2011.03.006.

[25] Rossetto T, Gehl P, Minas S, Galasso C, Duffour P, Douglas J, et al. FRACAS: A capacity spectrum approach for seismic fragility assessment including record-to-record variability. Eng Struct 2016;125:337–48. doi:10.1016/j.engstruct.2016.06.043.